Thermal Modeling of Tissue Ablation During Pulsed CO2 Laser Gingivectomy for Gum Reshaping and Reduction.

BEE 4530 - Computer-Aided Engineering:
Applications to Biomedical Processes

Ryan Bender, Michael Gross, Wenjie Luo, Emily Tess

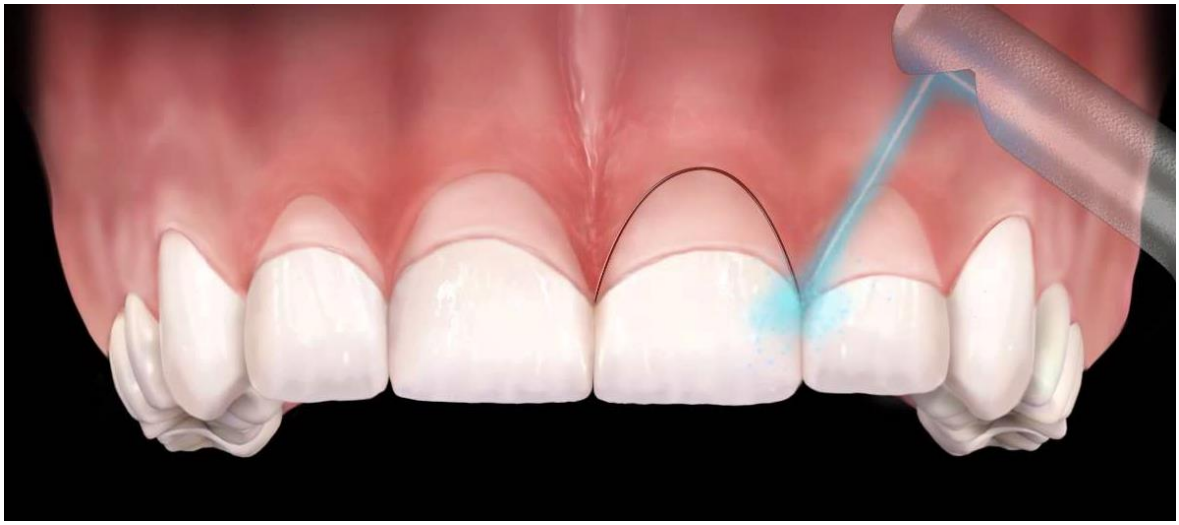

Table of Contents

Executive Summary

Gingivectomy, a surgical gum treatment used to remove gum tissue, is applied for a variety of reasons, including the removal of diseased gum tissue and gum contouring for aesthetic purposes. While a scalpel has been previously used in this procedure, laser gingivectomy is now becoming common due to its decreased invasiveness, minimal bleeding, and quicker healing time.

However, an entirely new set of considerations must be addressed with the introduction of lasers to the procedure. Since laser gingivectomy is essentially heat treatment, the heat from the laser can damage surrounding tissue and teeth. Therefore, the intensity of the laser beam must be carefully selected to prevent significant damage of teeth or non-targeted gum tissue above the incision line. A feature that helps preserve healthy tissue is the pulsed application of the laser, which prevents the exposure of the tissue to heat flux over an extended amount of time. Therefore, our goal was to model a laser gingivectomy process that may be used to identify the ideal laser power and pulse rate for gingivectomy that minimizes collateral tissue damage.

To accomplish this, we created a 2D cross-sectional model in COMSOL of the middle of a maxillary incisor with an overextending gum. The COMSOL computer software allowed us to simulate the effects of laser contouring on the gum-tooth complex. Gum geometry was simplified to a slab of constant thickness across the top of the incisor, meeting the tooth at a rounded edge. Tooth geometry was simplified to a series of rectangular slabs exhibiting constant thickness consistent with parameters gleaned from literature. Preliminary results showed little heat penetration to the extremes of our computational domain, which supports the simplification of not including the entire length of the tooth in our geometry.

Material properties, such as the thermal conductivity, density, and heat capacity of gum and tooth were taken from existing literature. We considered targeted gum to be vaporized at a temperature of 100˚C, consistent with surface soft tissue heat treatment characteristics. Ideally, tooth and preserved gum should stay below 60˚C. The tooth temperature profile is considered in an optimization equation that aims to minimize unnecessary tissue damage. This temperature profile is used to determine which regions are suffering protein denaturation and experiencing vaporization. By comparing our results with previously conducted procedures involving laser treatment of gum, we found that our results were consistent with the outcomes of these processes, which used the same type of laser as the one we modeled.

Noting that the simplifications and conjectures on boundary and initial conditions limit the validity of our model, our results indicated that the ideal laser peak power for a gingivectomy process using a CO_2 laser is 25 Watts. Our model could also be used to test the use of gingivectomy to dispose of diseased tissue, which likely exhibits different material properties than the healthy gum tissue we modeled. Therefore, our model can provide laser manufacturers and product trainers with crucial information that can be used to develop parameter settings for a more controlled gingivectomy.

In this study, we model the ablation of the gum tissue and find the optimal power of the laser and pulse conditions in order to successfully ablate the tissue without causing unnecessary heat damage to the healthy tissue or the enamel of the tooth.

1. Introduction

1.1 Background of Gingivectomy

The treatment necessary to correct an uneven gum line is called gingivectomy—the removal and contouring of gingiva. In the past, this was a painful process involving an injected local anesthetic followed by cutting the gums directly with a scalpel [1]. This procedure led to significant bleeding and required a long recovery period. Often, the painful procedure and recovery itself was enough to deter a patient from wanting to receive the treatment.

1.2 Therapeutic Laser Technique: A review of laser usage in modern medicine

The introduction of lasers to soft tissue surgical procedures has dramatically enhanced gingivectomy for both the surgeon and the patient by eliminating the scalpel and thus allowing for a faster, cleaner, and more pain-free procedure [1]. Typically, a laser emitting a far-infrared wavelength of light (10.6 μm) is used to cut soft tissue, such as the gingiva [2].

Many types of lasers have been developed for use in this type of oral surgery. Two common examples are the CO_2 laser and the diode laser. While the light emitted by CO_2 lasers is absorbed primarily by water, diode laser light is absorbed by melanin and hemoglobin proteins [1]. Therefore, diode laser light targets only pigmented tissues, leading to rapid heating in the gingiva. [3].

These lasers cut tissue with a phenomenon known as the *photothermal effect*: the light energy emitted by the optic fiber of the laser is transformed into heat in the soft tissue. As the tissue heats, chemical bonds between cells break down causing ablation of the tissue with simultaneous cauterization at the site where the cut was made [1]. This creates a clean cut with minimal bleeding and significantly reduced recovery time when compared to the traditional scalpel method.

We have chosen to focus in particular on the CO_2 laser, in which the wavelength is generated through the excitation of CO_2 gas [3]. These lasers have grown in popularity due to their advantages in providing minimal post-operative discomfort, little bleeding, and easier accessibility to areas of mouth [4]. Many of these advantages relate to their short penetration depth that focuses thermal tissue damage only on the surface of the tissue [3]. These lasers allow for very accurate cutting and do not involve the complex considerations involved with light scattering in more deeply penetrating lasers, such as the diode laser.

1.3 Modeling and Optimization Objectives

Since the laser wavelength is primarily absorbed by water, it targets the moist soft tissue of the gingiva more directly than the enamel of the tooth. However, the heat transfer through the healthy gum tissue and into the tooth itself must be considered and minimized in order to minimize postsurgical complications. A pulsing laser is ideal since continuous laser delivery often yields

suboptimal surgery results, with significant surrounding tissue damage caused by continuous energy delivery without time for heat dissipation [5] (see Appendix B). To minimize injury to healthy gum tissue, the peak power of the laser and pulsation frequency can be adjusted to reduce the temperature of surrounding tissue.

We aimed to ablate all targeted gum tissue, achieved by reaching 100^{o}C in all areas of this tissue, since 100^{o}C is the point at which tissue vaporizes [5] (see Appendix B). We aimed to successfully model the ablation of all targeted tissue while minimizing thermal tissue injury, as proteins denature significantly past 60^{o}C and tissues are considered damaged beyond this point.

In minimizing thermal tissue damage, we consider the temperature of the enamel, dentin and the untargeted gum tissue, which we defined as all gingival tissue above the incision line. Although a small amount of damage to untargeted tissue is inevitable due to the cauterizing effect of laser cutting, we want to minimize any additional potential loss of this healthy tissue. All gingival tissue below the incision line is removed during the procedure so we will not factor any thermal damage of this tissue into the optimization.

We created an objective function that calculated the area of the damaged tissue for different sets of parameters, giving higher weights to any enamel or dentin damaged. From this, we determined which combination of laser properties minimizes tissue damage.

1.4 Scope of Work

Our work in this project does not aim to develop a new technique for gingivectomy. The surgery has already been used successfully for many years. However, it has been implemented using many slightly varying techniques. We aim to focus on creating a model of the procedure to determine the optimum parameters of pulse type and peak laser power in an attempt to inform the potential for device advancement and manufacturing goals for future iterations of dental lasers.

2. Problem Statement

Since there is no existing model for laser gingivectomy of the maxillary incisor using a CO_2 laser, our goal was to create a 2D simulation in COMSOL to model the laser ablation of this tissue. Using this model, we planned to determine the optimal power of the laser and pulse conditions in order to successfully ablate the tissue without causing unnecessary heat damage to the healthy tissue or the enamel of the tooth. Our COMSOL simulation modeled the action of the laser beam by implementing a pulsed laser flux over a focused area of tissue. To assess tissue damage, we applied a binary temperature profile function to the results that clearly indicated damaged and undamaged tissue, to determine which laser power, and pulse conditions, can minimize damage to the healthy tissue outside of the targeted region.

3. Design Objectives

1) Develop a 2D model on COMSOL of upper central incisor with relevant layers of gingiva, enamel, and dentin.
2) Test 2D domain with time-dependent heat conduction model, implementing, for boundary conditions, a constant flux to a small surface section of the gingival tissue representative of the laser beam. We treat the targeted gingival tissue section as a changing geometry that shrinks with laser application, accounting for the removal of ablated tissue as the cut is made.
3) Modulate the laser flux for values consistent with current literature and practices.
4) Modulate the application of the laser, simulating pulsatile conditions by implementing laser flux as a square wave to compare against continuous application.

4. COMSOL Implementation Methods

4.1 Schematic of gum and tooth geometry

The right front maxillary incisor was chosen as a model for the study. Gingivectomy procedures are commonly done on the incisors, due to the high visibility of the front teeth. Figure 1 shows the abstraction and generalization of geometry from the mouth to a two dimensional graphic.

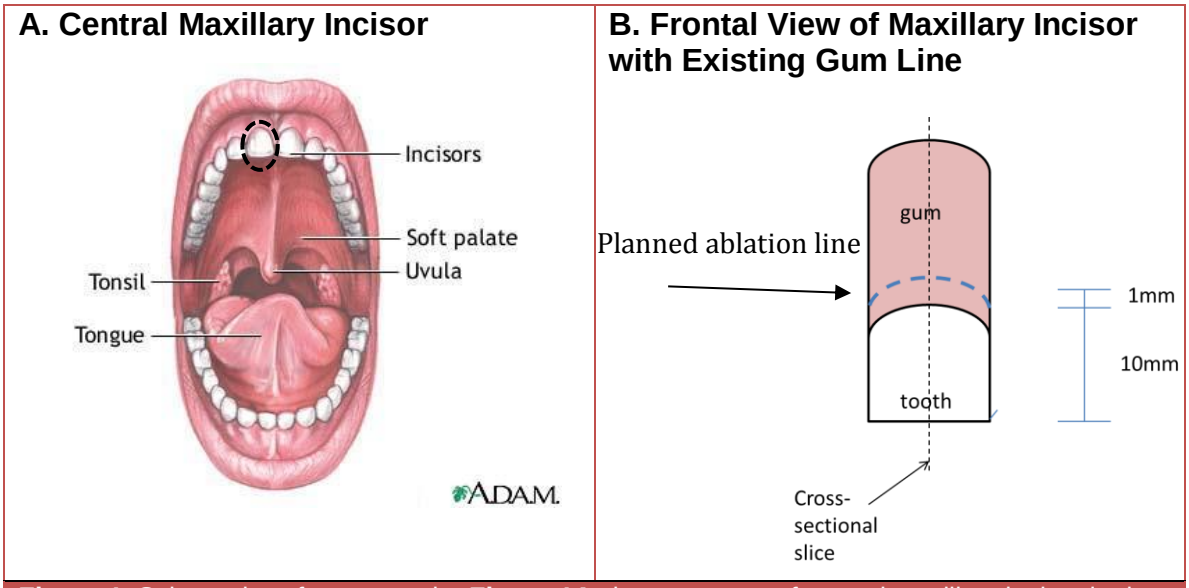

Figure 1. Schematics of target tooth. **Figure 1A** shows context of central maxillary incisor in the mouth. [6] **Figure 1B** is a simplified geometry of the frontal view of the central maxillary incisor showing the existing gum line and the planned line of ablation for gum trimming.

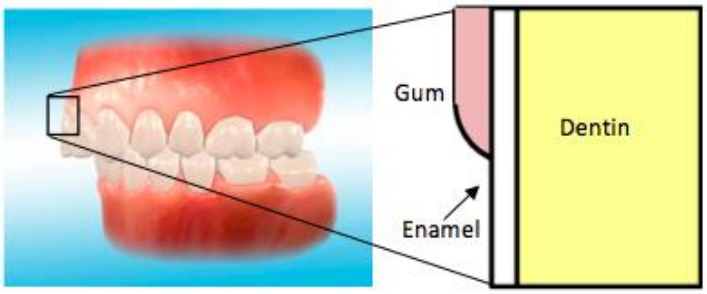

Figure 2. Simplified geometry of cross-section of incisor [7] (indicated by dotted line in **Figure 1B**) with gum, enamel, dentin and pulp represented by different sections.

Using population averaged values [8] for the average thickness of gum, enamel, and dentin, we constructed a theoretical two dimensional cross-section of Figure 1B above, shown here in Figure 2. The ablation of tissue will take place 1mm above the start of the gum tissue and will proceed as shown in Figure 3.

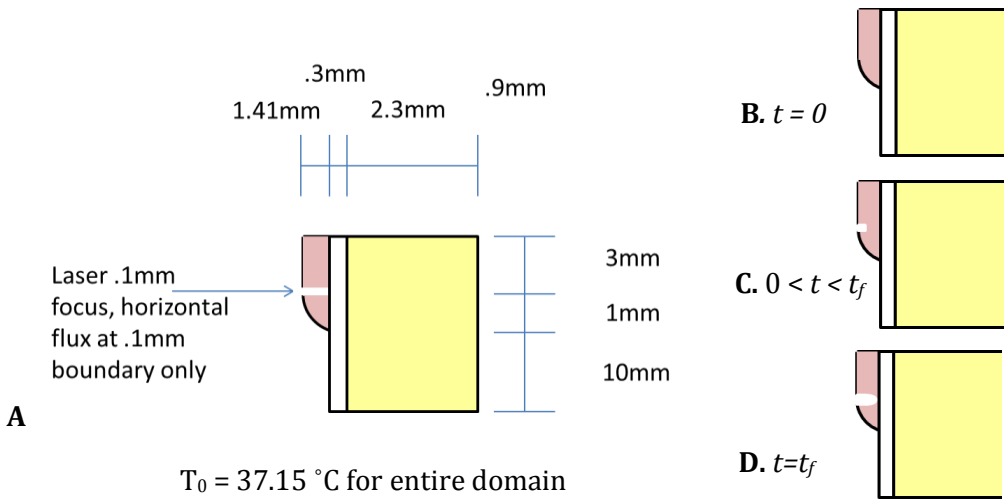

Figure 3. A: Simplified geometry of cross-section (indicated by dotted line in **Figure 1B**) of incisor with gum, enamel, dentin and pulp represented by different sections from the left with boundary conditions included (flux only at ablation rectangle, all other exterior surfaces insulated)**. B, C, D**: A proposed progression of heating along the simplified geometry at **(B)** start of the procedure, **(C)** mid –ablation time, **(D)** end of procedure. Values were from population averages [8].

4.2 Mesh implementation in the gum and tooth domains

Using COMSOL, a mesh was constructed of free triangular elements as shown to the right. Meshing in the gum layers was tailored to be finer than the enamel or dentin layers due to their large geometries and the observed lack of substantial heat penetration into those layers. This variation in mesh density for different regions is shown in Figure 4.

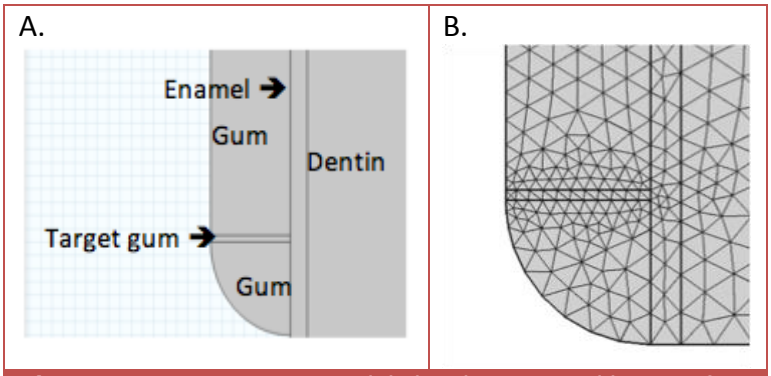

Figure 4A: 2D COMSOL model showing cropped image of model. **Figure 4B**: A free triangular mesh of the tooth and gums, using a "normal" mesh with a total of 581 mesh elements.

Mesh convergence:

Using temperature versus time plots of different sized meshes at different points within the ablated and surrounding tissue, the maximum mesh size needed was found to be at COMSOL's predefined "coarser" mesh with 509 total mesh elements. This is because the temperature versus time plots begin to diverge once an "extra coarse" mesh is used (472 elements). As indicated in Figure 5, temperature changes over time at points within as well as outside of the ablated gum tissue region show that temperatures only being to diverge at the "extra coarse" mesh.

However, though our temperature values converged at a "coarser" mesh, our moving boundary condition encountered complications with this mesh. In order to avoid inverted mesh element errors and ensure that our stop condition yielded an accurate solution with a realistic geometry, the implementation of the moving boundary required that we use an "extremely fine" mesh, with 7304 total mesh elements.

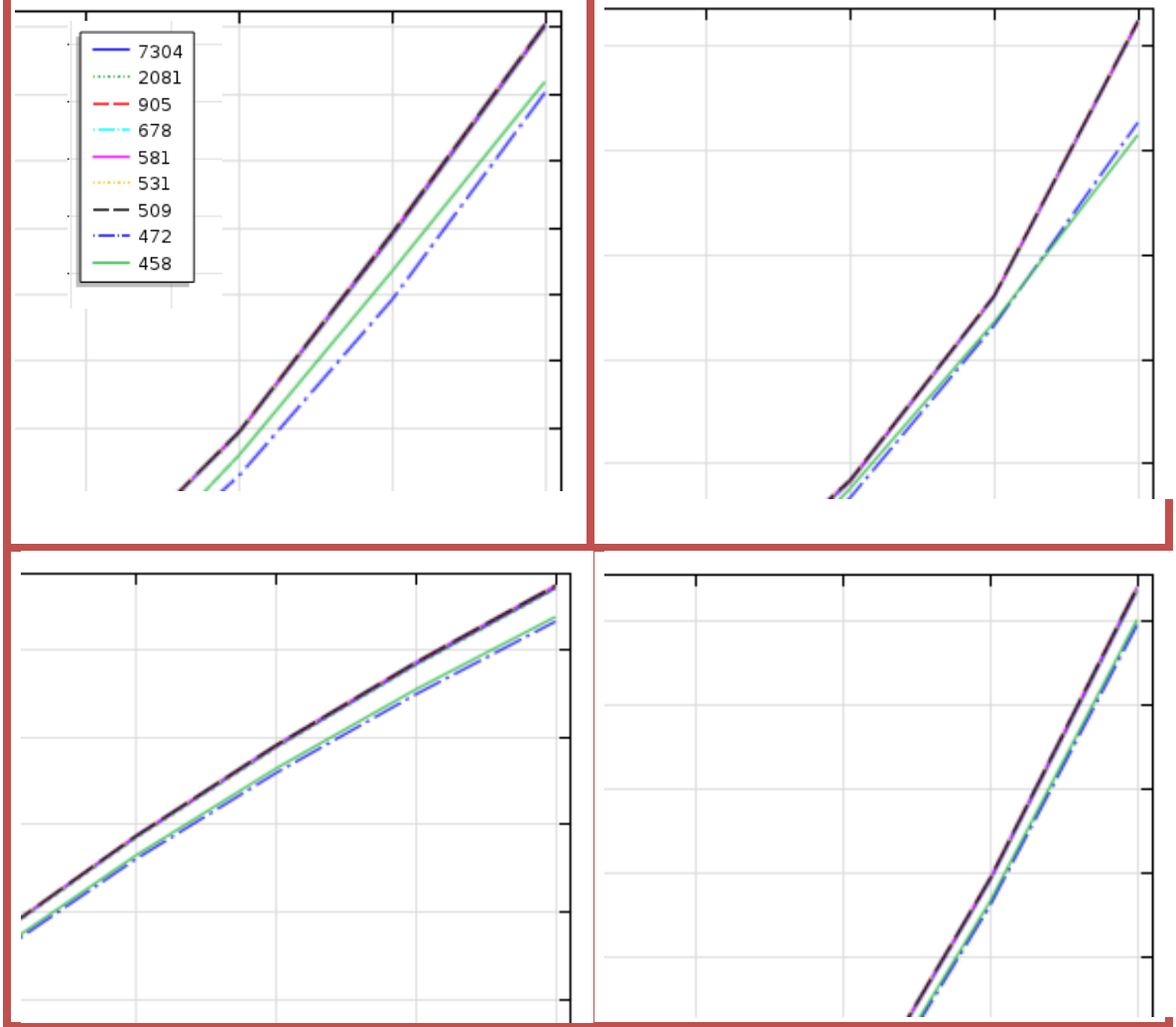

Figure 5. Zoomed plots of temperature vs. time at four different points in the gum tissue. Each colored line represents the solution at a different predefined mesh in COMSOL. The legend denotes the number of mesh elements that corresponds to the predefined mesh. See Appendix for figures of the entire plot as well as the point in the geometry from where this data was taken.

4.3 Equations governing heat transfer and the moving boundary

The following governing equation was used in the study to model the diffusion of heat from the laser through the tissues in two dimensions.

$$\frac{\partial T}{\partial t} = \frac{k}{\rho C_p} \nabla^2 T \tag{1}$$

We ignore any convection or heat generation within the tissue since they have an inconsequential impact on the overall heat transfer of this model given the time scale and order of magnitude of the flux. The function of biological heat generation is to keep the body at room temperature. As

our laser is heating tissues to above 100˚C, the heat generation maintaining the body at 37˚C has a comparatively small magnitude that does not have an impact on our solution during the short time scale (hundreds of milliseconds).

Equation 2 describes the velocity, in the x-direction, of the ablation front of the tissue using a CO_2 laser of wavelength 10.6 μm. Due to the large wavelength, the laser only penetrates 10 μm into the tissue [3] allowing us to make the assumption that the laser light has no penetration depth and treat the laser as a constant flux surface boundary condition.

$$v = \frac{\Phi_0}{\rho(C_p \Delta T + L)} \tag{2}$$

We will use a moving boundary condition that simulates the shrinking of the tissue as it is ablated with the above velocity, where v = speed of cut (m/s), ϕ_0 = laser fluence, (W/m^2), ρ = density of tissue (kg/m^3), C_p = specific heat of tissue (J/kg K), ΔT= 100-37 = 63K, and L = latent heat of vaporization (J kg^{-1}) [3]. The high water content of soft tissue allows its property values to be approximated as equal to the values of water [9].

In COMSOL, this velocity equation was implemented on the surface of the targeted region and is only in effect when T > 100˚C as this is the temperature at which tissue will vaporize.

The computation was run until a general stop condition was reached similar to how a laser operator would know to cease ablation when minimal gum remains in the incision site to avoid incising the enamel. The compiler terminates once the target region has reached 2% of its starting area. An example of the coding node for this feature can be seen in Figure A5 in the Appendix.

Our preliminary model also included a thermal damage equation (Equation 3) to assess the soft tissue damage in the gum. We attempted to model gingival tissue damage (Ω) through the following equation.

$$\frac{d\Omega}{dt} = A * e^{\left(-\frac{E}{RT}\right)} \tag{3}$$

In the above equation, parameters A and E represent experimental parameters for thermal tissue injury. However, the solution to Equation 4 was ultimately not used in our analysis due to the fact that it yielded unrealistic results as COMSOL was unable to compute correctly using the parameters that we found for such a small geometry.

4.4 Boundary Conditions

We implemented the following boundary conditions in our model based on the assumptions stated below.

1. Heat flux on the ablation surface of the moving boundary: $\phi = 3.1831E9\ W/m^2$. The tissue should vaporize at 100^{o}C on this surface, thus causing any mesh that reaches 100^{o}C to be reduced in size corresponding to the velocity mentioned above.
2. We assume a heat flux of 0 W/m^2 on the upper, lower and right-most boundaries of our model.

3. We assume a heat flux of 0 W/m^2 at the gum surface not exposed to the laser.

The flux on the ablation surface is implemented as a square wave with a pulse of high intensity laser light and an interim period without laser light to model the pulse of the laser. This pulsation of flux allows time for heat to dissipate in the tissues, leading to lower temperatures throughout the domain [5] (see Appendix B).

4.5 Initial Conditions

We assumed that the entire system is at 37°C initially, normal body temperature.

4.6 Input parameters

The average thermal properties in the three layers of our domain are shown in Table 1 below.

Table 1. Thermal properties of gum, enamel, and dentin tissue as found in literature search.

Thermal Properties of Teeth				
	Parameter	**Value**	**Units**	**Reference**
Gum	α	1.50×10^{-7}	m^2s^{-1}	[9]
	ρ	1.00×10^{3}	kg m^{-3}	[9]
	k	0.63	W m^{-1} K^{-1}	[9]
	C_p	4.20×10^{3}	J kg^{-1} K^{-1}	[9]
Enamel	α	4.69×10^{-7}	m^2s^{-1}	[10]
	ρ	2.80×10^{3}	kg m^{-3}	[10]
	k	0.93	W m^{-1} K^{-1}	[11]
	C_p	0.71×10^{3}	J kg^{-1} K^{-1}	[10]
Dentin	α	1.87×10^{-7}	m^2s^{-1}	[10]
	ρ	1.96×10^{3}	kg m^{-3}	[10]
	k	0.58	W m^{-1} K^{-1}	[11]
	C_p	1.59×10^{3}	J kg^{-1} K^{-1}	[10]

The use of the square wave to model the laser pulse yields three fundamental laser parameters: peak power (used to determine the height of the square wave), pulse frequency, and pulse length (the portion of a period that the laser is actually on).

Table 2. Input parameters for CO_2 laser properties.

Laser Parameters			
Parameter	Value	Units	Reference
Laser Power	10	W	[12]
Frequency	20	Hz	[12]
Pulse Length	.005	s	[12]

4.7 Optimization of the solution

We created an objective function for optimization based on a binary state of damaged vs. undamaged tissue for all areas of the model by labeling any healthy tissue that reached 60˚C as damaged. Once the tissue reached the threshold for protein denaturation and was considered damaged, any further increase in temperature was not pertinent to our analysis. The objective function was created based on the integration of the binary temperature plots over time. The binary plots were integrated over the damaged area (greater than or equal to 60˚C).

These integrated values were then used as the independent variable in our objective function. The higher the output value of the objective function was, the less desirable the situation. We then scaled the integrated values based on domain. The integrated value of the binary value of the gum tissue is not scaled at all. That occurring in the enamel is multiplied by 100, and that occurring in the dentin is multiplied by 1000. This was done in an attempt to place extra sensitivity of the objective function on those regions that were of more importance not to damage. Though we aimed to minimize all tissue damage, damage occurring past the gum, and especially in the dentin, should never occur as a result of this procedure.

Therefore, high values of the objective function associated with damage occurring in the enamel and dentin will ensure the solution is not optimized using parameters that allow for large damage past the gum. The optimized solution is the function exhibiting the lowest value of the objective function and completed in the shortest span of time. Equation 4 below is the specific objective function that we wish to minimize.

$$J = \sum_{gum} \begin{cases} 0, & T < 60 \\ 1, & T \geq 60 \end{cases} + \sum_{enamel} \begin{cases} 0, & T < 60 \\ 100, & T \geq 60 \end{cases} + \sum_{dentin} \begin{cases} 0, & T < 60 \\ 1000, & T \geq 60 \end{cases} \qquad (4)$$

Additionally, since the stop time is based on the reduction of tissue size, each parameter change will likely affect the stop time for that simulation. Thus, a second dependent variable, the stop time, should be accounted for, as well as the objective function. Since the time is less important than the tissue damage, however, this variable will not be used extensively for decision making about the optimal parameter settings. Rather, this variable will be used to qualitatively analyze our setting decisions, so that we can obtain a general sense for how much time such a procedure would take.

By varying parameters, we created many sets of binary plots to be utilized in our objective function. Modulation of the parameters of the pulsed wave function (peak power, duration of pulse, and pulse length) allowed us to conduct our optimization process as well as determine the sensitivity of our equation to each of these variables.

We ran a parametric sweep with different values for three parameters: pulse power, pulse length, and frequency. In order to execute a parametric sweep, it was necessary that we knew our range of allowable values based on the physical constraints of our system.

For laser power, values were selected in the same clinically relevant range that is currently used by dentists. For CO_2 lasers, the optimum power level seen in the literature was 10 W. [12] Additionally, a typical CO_2 dental laser can only reach a power of 25 W [13]. Therefore, we used the values 5, 10, 15, 20 and 25 in order to give a range around the clinically used laser power values.

For continuous wave lasers like the CO_2 laser, a mechanical shutter is used to break up the laser into separate pulses. The optimal CO_2 laser pulse duration was found in the literature to be 0.015 s [12] so we tested values between these two. Therefore, we ran simulations at 0.005, 0.015, 0.025 and 0.05 s pulse lengths.

We based our frequency on the existing data for laser gingivectomy treatments. The most common frequencies seen in these surgeries with diode lasers are 15 and 12 Hz [5] (see Appendix B); however, 20 Hz was considered the optimal for CO_2 lasers [12]. Therefore, we will set up frequencies of 5, 10, 15, 20, and 25 Hz.

These values give us a bit of range around the clinical values, to allow us to explore a greater number of parameter combinations. The results of the optimization of our solution can be seen in Figure 6. Surprisingly, only laser power seemed to have an effect on the results (this will be discussed later). As such, only laser power was optimized in Figure 6, as Figures 7 and 8 showed that frequency and pulse length variations did not affect the objective function.

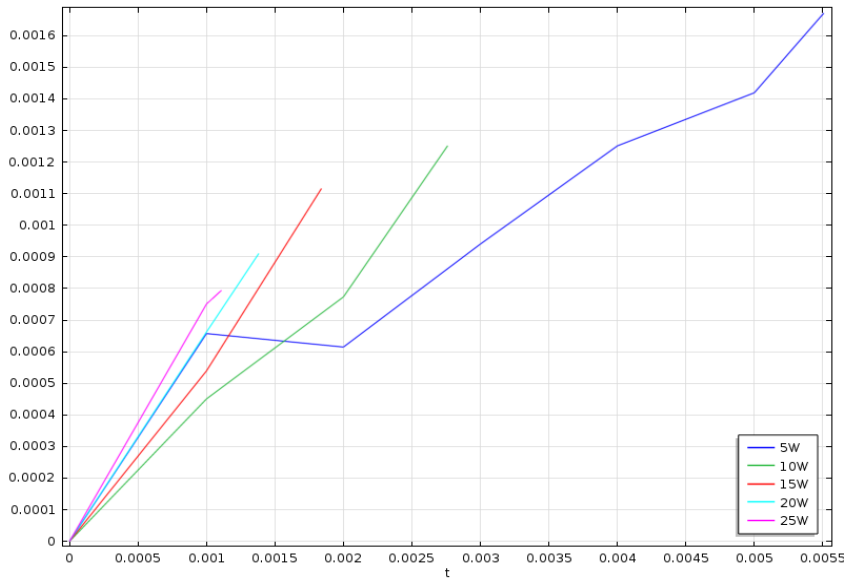

Figure 6. Objective function over time for varying laser powers. Using this plot, 25 W was shown to be the optimal laser power as it exhibits the lowest objective function value and also completes the simulation in the shortest amount of time.

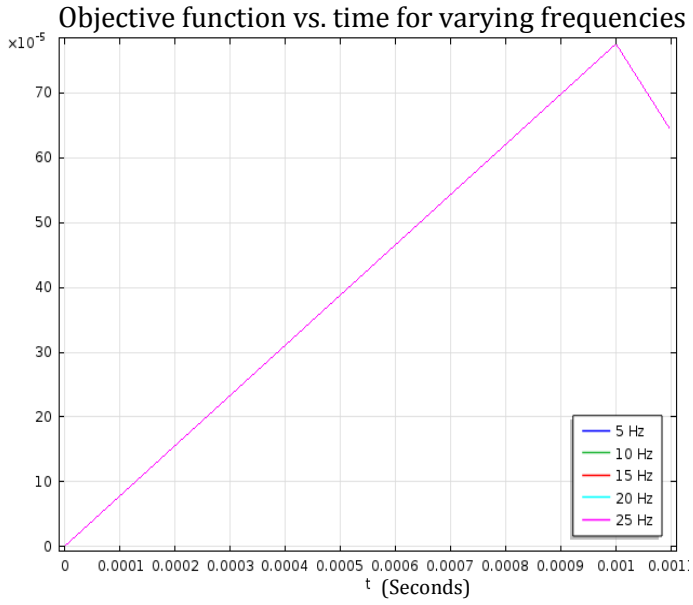

Figure 7. Objective function over time for varying frequencies, all at a laser power of 25 W and with pulse length 0.005 s. The overlapping of the different functions shows that frequency variation does not affect the objective function and therefore is not considered in optimization.

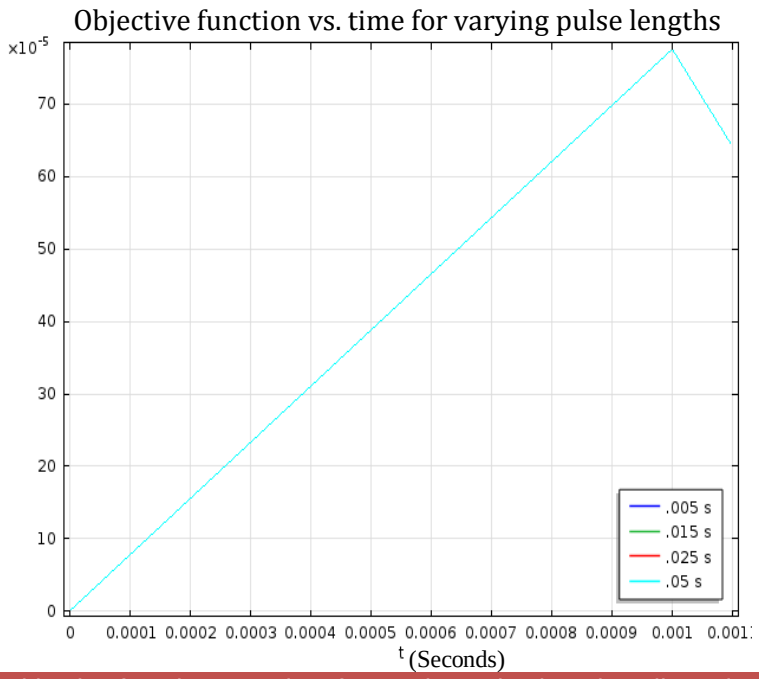

Figure 8. Objective function over time for varying pulse lengths, all at a laser power of 25 W and with frequency 20 Hz. The overlapping of the different functions shows that pulse length variation does not affect the objective function and therefore is not considered in optimization.

4.8 Sensitivity Analysis

Sensitivity analysis of the parameters for material properties was performed. As previously mentioned, gingivectomy can be used to remove diseased gum tissue, which can often have thermal properties that differ from that of normal gum. Therefore, a parametric sweep was conducted on COMSOL on the material properties of the gum tissue (density, thermal diffusivity, thermal conductivity, and specific heat) for +/- 10% of the literature-defined value.

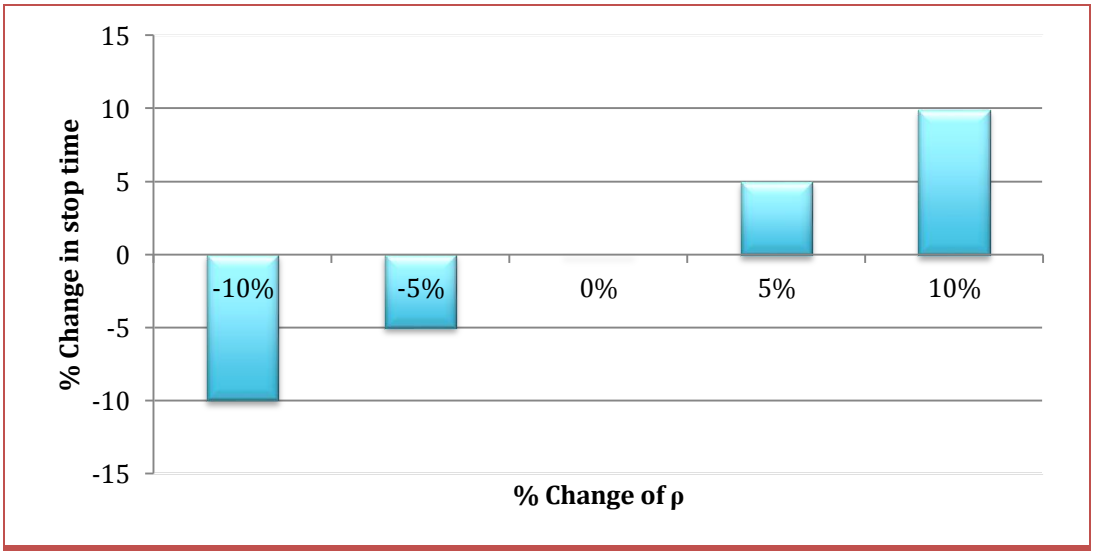

Figure 9. Sensitivity of the gum density ρ on the time it takes to complete the ablation of the gum at a single point.

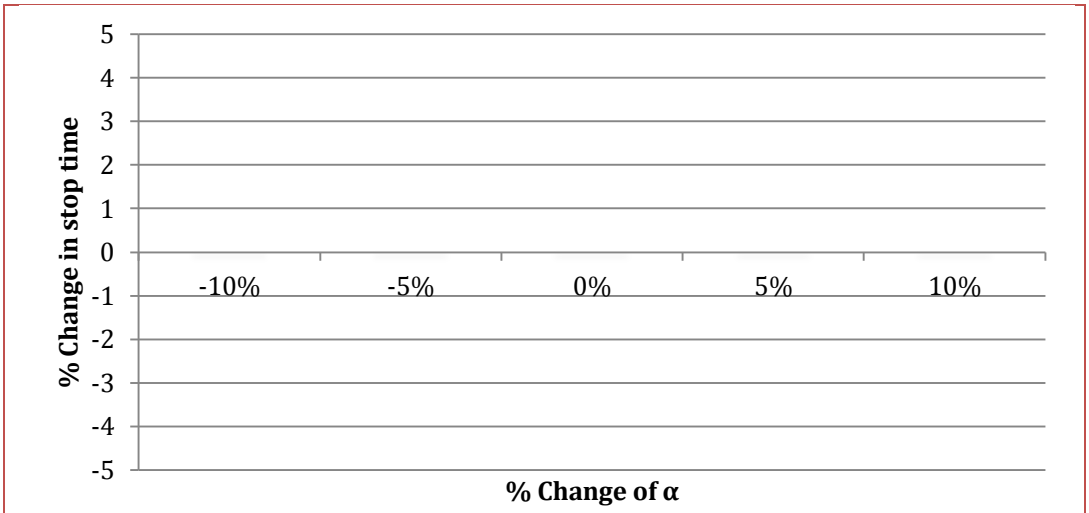

Figure 10. Sensitivity of the gum's thermal diffusivity α on the time it takes to complete the ablation of the gum at a single point

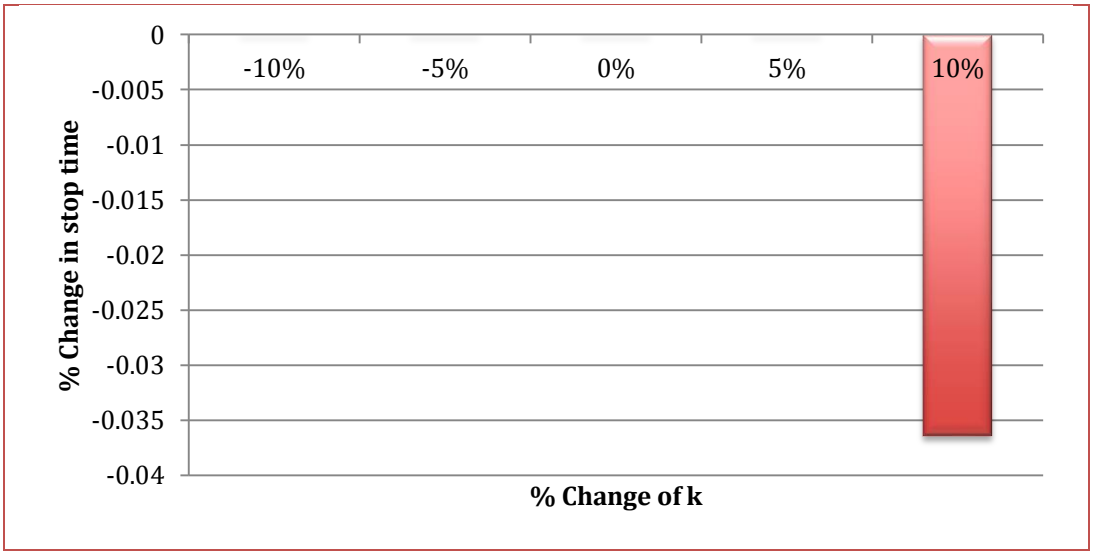

Figure 11. Sensitivity of the gum's thermal conductivity k on the time it takes to complete the ablation of the gum at a single point.

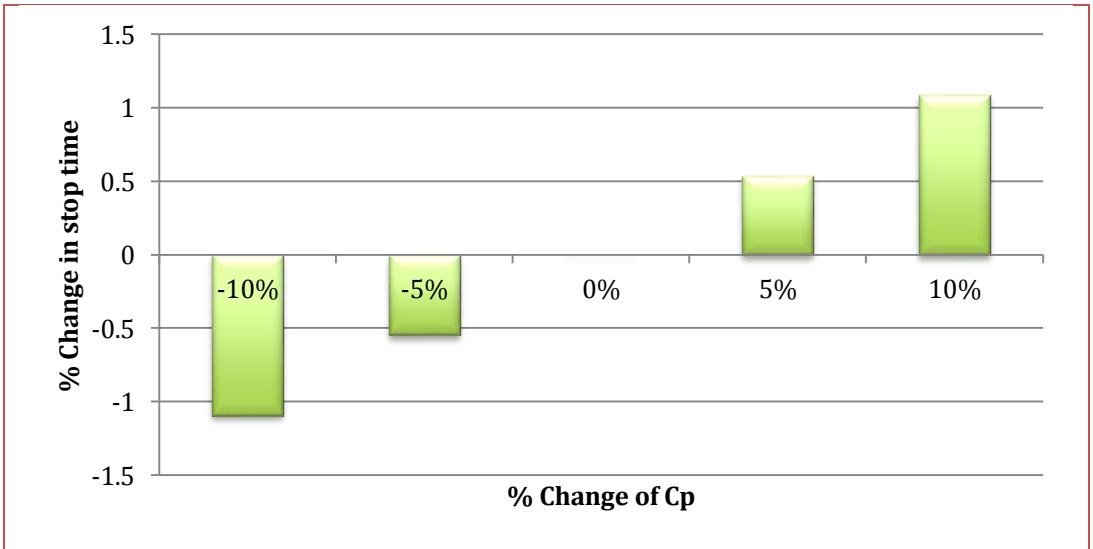

Figure 12. Sensitivity of the gum's specific heat c_p on the time it takes to complete the ablation of the gum at a single point.

Two of these four parameters proved to affect the completion time, gum density and specific heat, which can be seen in Figures 9 through Figure 12.

5. Results and Discussion

The model performed amicably and the desired tissue ablation was achieved even in preliminary implementations of the simulation. For instance, in Figure 13, we see the controlled movement of the 0.1 mm boundary face as the tissue heats due to a constant laser flux on that surface. The time for this simulation to complete was 7.56 seconds using a flux of 81.5 W/cm^2.

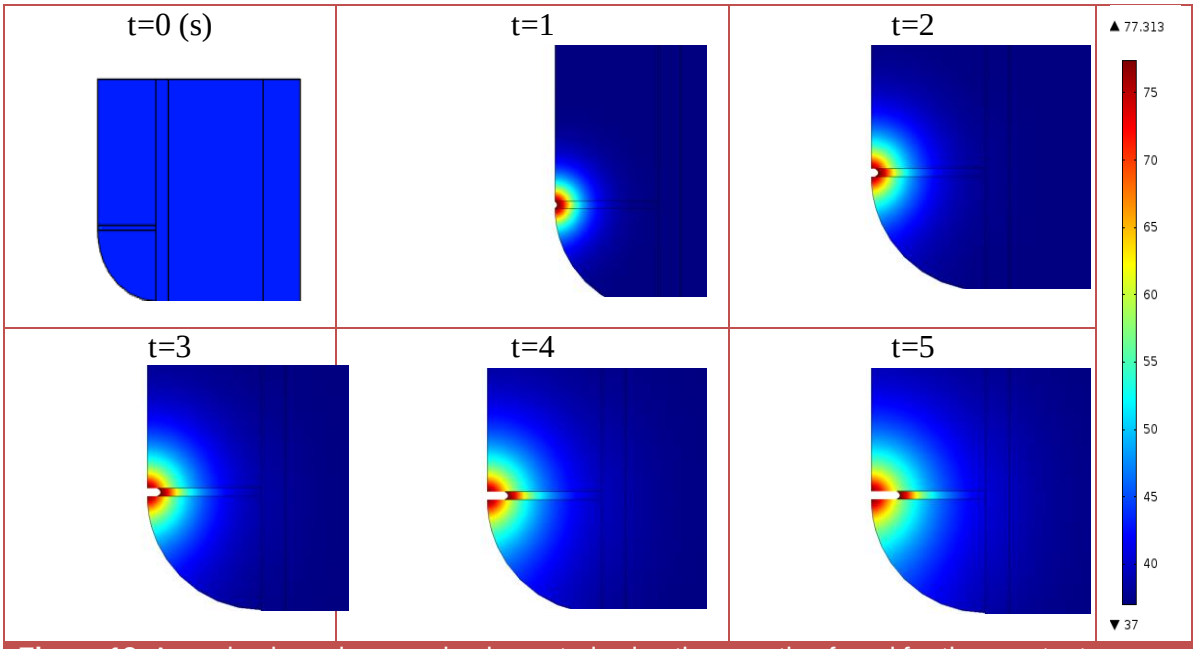

Figure 13. A moving boundary was implemented using the equation found for the constant velocity of tissue ablation due to laser heating in soft tissue. The rectangle in the center represents the tissue that is ablated.

When examining the temperature profiles in Figure 13, we see some spreading collateral damage in the surrounding, untargeted, gum layers as temperatures reach 60 ^{o}C and above, but it does not appear to impact the overall geometry of the region. This means that no tissue outside of the ablation zone exceeded the 100˚C temperature necessary for ablation.

Although the targeted gum tissue reaches temperatures in the ablation range (>100^{o}C), some of the surrounding healthy gum tissue reaches high temperatures, especially around time = 3 s. The surface of the healthy gum tissue surrounding the ablated section is the part of the gum exposed to the most heat and, in this region temperatures reach values that would lead to charring of tissue. Looking at the final temperature profile, sections of the enamel and dentin do have increased temperatures from their initial state. Fortunately, the temperature of the sensitive dentin of the tooth remains in the healthy region suggesting no thermal damage.

Following these preliminary results, we then implemented the clinical levels of laser power, ultimately analyzing the "optimal" power of 25W. Figure 14 shows the temperature profiles generated using this laser power of 25 W and a pulse length of 0.005 seconds.

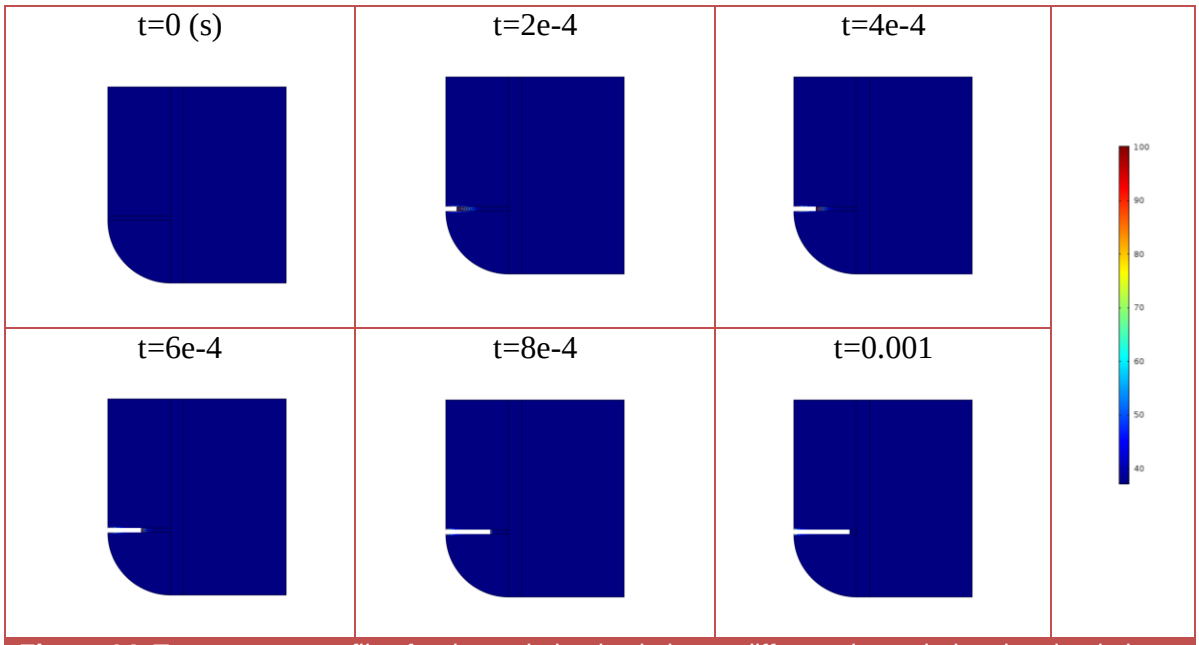

Figure 14. Temperature profiles for the optimized solution at different times during the simulation process in degrees Celsius.

By comparing Figures 13 and 14, it is clear that less heat dissipation is observed in our final model and the simulation is also completed in a much shorter time (7.56 seconds vs. 0.001 seconds).

Figure 15 shows a plot of the COMSOL results from the tissue damage equation we had initially implemented as a transport of diluted species physics. However, as some of our input values were on a very large order of magnitude, the solution didn't evaluate correctly and yielded incorrect results. Instead, we used the binary determination, marking tissue as damaged as soon as 60˚C has been reached.

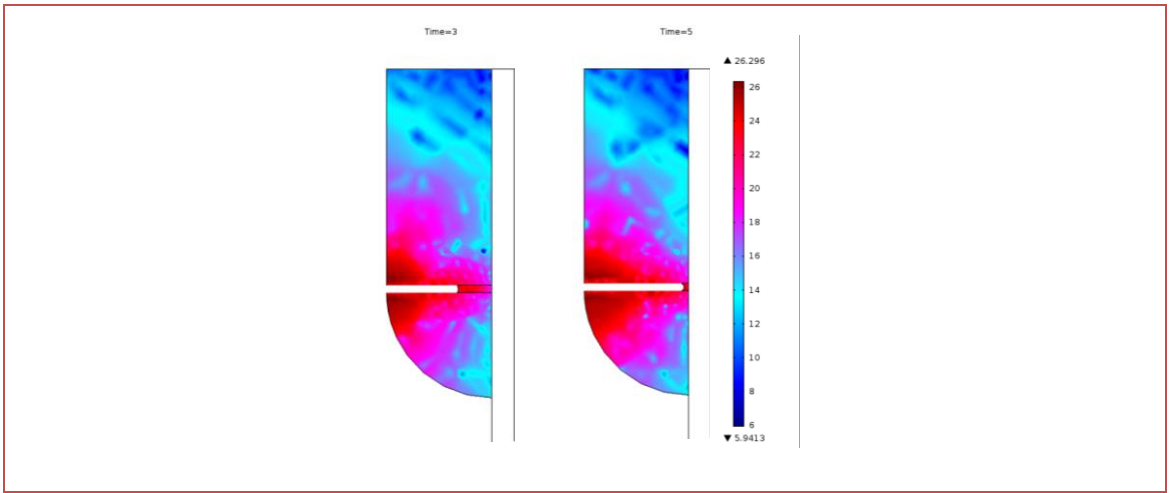

Figure 15. Thermal tissue damage, omega, based on COMSOL implementation of Equation 4 in gum layers only. Time given in seconds. Because values of omega should be between 0 and 1, this plot shows results that do not give an accurate representation of tissue damage. Therefore, we did not proceed with the analysis of this data.

5.1 Validation of Model

Though initially concerned about the very small timescale in which our experiment came to completion, we found that an existing surgical video of the CO_2 laser gingivectomy procedure suggested that 1ms might actually be a valid result. The video that we found [14] shows a laser gingivectomy procedure, in which gingival tissue is ablated from the mouth of a patient Between 0:44 and 0:49s, the dentist ablates the gum tissue of one central maxillary incisor, but, in doing so, he makes several passes over the tooth, making it difficult to determine the exact amount of time to complete a pass over any easily determined length of tissue. Between 0:48 and 0:49, a stopwatch was used to determine that the dentist ablates a section of tissue roughly equal in length to one half of the tooth-gum arc length in 0.5 s. This generates a procedure time per tooth, for one pass with full ablation, of 1 second per tooth.

In the literature, it was found that for an adult male, the width of the anterior dentition for the maxillary incisor had a mean of 8.0 mm [15]. Treating the tooth-gum arc length as a semi-circle with diameter 8 mm, we determine that the arc length is 12.57 mm. Since the laser we modeled has a diameter of 0.1 mm [16], it would take roughly 126 of the ablations seen in our simulation to ablate the tissue of the entire tooth-gum arc. Applying the stop times generated for the 5 laser power levels we tested, we get procedure times that can be seen in Table 4.

Table 4. Calculations of procedure times for various laser power levels.

Power Level	Time to complete Simulation	Time per tooth
5 W	0.0055 s	0.693 s
10 W	0.0028 s	0.353 s
15 W	0.0018 s	0.227 s
20 W	0.0014 s	0.176 s
25 W	0.0012 s	0.151 s

Literature values suggest that 10 W is optimal for surgical CO_2 laser settings, and, with these settings, we would expect the procedure to take 0.353 s. While this value is slightly less than half that seen for the ablation done in the video, it is worth noting that several features of the technique used in the video would cause the procedure to take longer. We had found that the highest flux values generated the lowest values of our optimization function, corresponding to the lowest amount of thermal damage to surrounding tissue. In the video, it is apparent that significant thermal damage is occurring to surrounding tissue as the gum tissue chars quickly after application of the laser, so it not unreasonable to suggest that lower laser fluxes are being used, and these fluxes would cause the procedure to take more time.

In addition, the dentist uses a water jet to cool the gum surface while performing the procedure. A convective cooling boundary condition could have massive effects on the procedure and could very reasonably slow the procedure. Perhaps most importantly, any water in the path of the laser would strongly absorb its energy, since CO_2 lasers' mechanism for tissue ablation is water

molecule excitation [3]. Such absorption would likely cause a significant decrease in the laser power actually delivered to the tissue.

This is an area for further research, but, unfortunately, due to the complexity involved with the addition of a water jet, we could not perform the research ourselves. Modeling a water jet would have to take into account water application velocity, water temperature, angle of water jet application, velocity of deflected water, and water accumulation, both on the surface of the gum tissue and within the constantly growing incision. In addition, this excess of water could yield a significant amount of steam upon vaporization, and this steam could cause unforeseen thermal effects on the tissue, as well as bringing in complications related to steam expansion.

Also, it is very reasonable to expect that it would be impossible for a dentist to operate with a flux so high that the procedure would take 1 ms to ablate the tissue at a given point. Such a high flux, and such a short ablation time, would challenge the dentist to make sure that the beam never touched the same area of gum tissue for more than one pulse, as the first pulse would fully ablate the tissue, and any subsequent pulses would damage the enamel. As such, it makes sense for dentists to use lower flux values, even though it causes more gum tissue thermal damage because of the larger time given for heat to diffuse to surrounding tissue.

The dentist is seen to scan across the tissue quite quickly during this procedure. Such application of the laser would cause less focused heating than the stationary method, which we modeled in our simulation. This would, therefore, cause the procedure to take a greater time, and it would cause our simulation to be less accurate, due to the additional cooling of tissue at the ablation site as the laser scanned to a different area of the tooth.

Following our optimization results for laser power, we discovered that the stop condition was being reached in about 1 ms. While we were able to verify this timescale with respect to the overall length of the procedure, we were not sure that this particular pulse length would be attainable using current technology. Our original minimum pulse length was 5ms, and if that was the case, a 25W pulse could not be used as it would expose the tooth to another 4ms of heating after the gum was successfully ablated. Fortunately, we were able to discover the existence of a CO_2 laser that can attain a pulse length of 1 ms [16]. This suggests that procedures using such low pulse times are possible, and, indeed, intended for use, specifically, as mentioned in the laser's product description, for "char-free" gingivectomy procedures.

For a secondary means of determining that our solution is accurate, we compared the volume of water that would be vaporized by the laser energy to the actual volume of gum that was ablated in the model.

In the COMSOL model, it takes 0.001 seconds for the tissue to be ablated all the way through the gum tissue. Using the optimized laser power of 25 W, a total of 0.025 J of energy are used to ablate the tissue.

Considering the following properties of water, the mass and volume of water starting at body temperature that would be vaporized by this laser energy can be determined.

Table 5. Thermal properties of water.

Properties of Water	
Specific Heat of Water	4.18 J/g˚C
Heat of Vaporization of Water	2257 J/g
Density of Water	1000 kg/m3

The following equation can be used to estimate the mass of water that would be vaporized given the energy from laser flux.

$$Energy = mc\Delta T + m\Delta H_f$$

This estimation yielded a volume of 0.0099 mm^3 of water vaporized. Considering the .1 mm spot as the diameter of the laser, a total of 0.01107 mm^3 of gum tissue is ablated in our actual model. There is a 10.6% error in the calculated volume of water that would be vaporized by the laser energy to the volume of tissue actually ablated in our model. It is expected that the volume ablated in the model would be less than that of the water. The difference is accounted for in the fact that gingiva is a soft tissue and biological material and not completely comprised of water. Also, the laser flux is not constant across this time, and instead is applied in a pulse, which would result in less volume vaporized. This indicates that our solution is valid.

6. Conclusion

By conducting the previously mentioned optimization procedure, the performance of the CO2 laser that we modeled was found to be optimal at a power of 25 W. Since the pulse lengths we tested only went as low as 0.005 seconds, the pulse length and frequency proved to be unnecessary to optimize as our model was fully ablated within one pulse length. In other words, regardless of the pulse length or frequency, the laser was always "on." Further research allowed us to find a laser that accommodated both a 25W power and the reduced 1 ms pulse length observed in our optimal solution. We had originally anticipated that a lower flux value would have the least amount of thermal damage, but take longer to ablate the necessary tissue. In analyzing our optimal result, it can be considered that the higher flux completes the simulation in a faster time and does not allow as much time for the heat to diffuse as compared to the lower flux solution. Although this is theoretically the optimal solution that yields the least tissue damage, in practice it may not be best as it requires a dentist to work very quickly in order to not hit the same spot twice and begin heating the enamel. Finally, the use of our model as a whole provided a strong case for the use of multiphysics engines to model those problems or procedures without the need to perform physical experimentation.

7. Limitations

The greatest limitation in the proposed model is the method by which we considered tissue ablation and subsequent vaporization. In our model, the boundary relating to the impact surface of the laser was limited to moving in the x-direction at a given velocity, provided the temperature at the boundary is 100˚C. We observed heating in our solution of those surrounding tissues, over 100˚C, that were not permitted to recede. Allowing for this could potentially change the final geometry and would have to be considered in an objective function

One of the greatest limitations of the study was the parameters and scale of our model. We worked with extremely large fluxes applied over an extremely small area which proved to be fairly computationally intensive and resulted in a number of "bugs" and unsuccessful compilations of the solution that retarded progress and expansion into new areas or facets of our study.

Finally, there was a significant suspicion in the group that the edge of our receding geometry was wrongly coupled to the corners of the boundary gum to which it was originally attached. This resulted in extreme heating of the corners of the domain and less heating above and below the ablation front as was expected. We consider this a bug in COMSOL's coupling protocol and plan to report it to their troubleshooting staff.

8. Future Work

A convective cooling boundary could be considered to further minimize tissue damage. Additionally, the use of lasers other than a CO2 laser to perform gingivectomy can be explored. For instance, a diode laser has a deeper penetration depth than a CO2 [5] and this diffusion of light and heat will need to be modeled by employing multiple physics. Were this to be implemented, the advantages and disadvantages to using certain lasers could be assessed by comparison of the optimized solutions generated by different laser models.

Appendices

Appendix A

Table A1. Input parameters

Parameter	Variable Name	Value
thermal diffusivity of gum	a_gum	$1.50 * 10^{-7}\ {}^{m^2}/_{s}$
thermal diffusivity of enamel	a_enamel	$4.69 * 10^{-7}\ {}^{m^2}/_{s}$
thermal diffusivity of dentin	a_dentin	$1.87 * 10^{-7}\ {}^{m^2}/_{s}$
thermal diffusivity of pulp	a_pulp	$1.50 * 10^{-7}\ {}^{m^2}/_{s}$
density of gum	p_gum	$1.00 * 10^{3}\ {}^{kg}/_{m^3}$
density of enamel	p_enamel	$2.80 * 10^{3}\ {}^{kg}/_{m^3}$
density of dentin	p_dentin	$1.96 * 10^{3}\ {}^{kg}/_{m^3}$
density of pulp	p_pulp	$1.00 * 10^{3}\ {}^{kg}/_{m^3}$
thermal conductivity of gum	k_gum	$0.63\ {}^{W}/_{m * K}$
thermal conductivity of enamel	k_enamel	$0.93\ {}^{W}/_{m * K}$
thermal conductivity of dentin	k_dentin	$0.58\ {}^{W}/_{m * K}$
thermal conductivity of pulp	k_pulp	$0.63\ {}^{W}/_{m * K}$
specific heat of gum	Cp_gum	$4.20 * 10^{3}\ {}^{J}/_{kg * K}$
specific heat of enamel	Cp_enamel	$0.71 * 10^{3}\ {}^{J}/_{kg * K}$
specific heat of dentin	Cp_dentin	$1.59 * 10^{3}\ {}^{J}/_{kg * K}$
specific heat of pulp	Cp_pulp	$4.20 * 10^{3}\ {}^{J}/_{kg * K}$
Fluence of laser	phi0	$81.50*10000\ {}^{W}/_{m^2}$
temperature change	deltaT	100-37 K
Energy mass ratio	L	$2.26 * 10^{6}$ J/kg
speed of boundary	v	phi0/(p_gum*(Cp_gum*deltaT +L)) m/s
Universal Gas Constant	R	$8.314\ {}^{J}/_{mol * K}$
Ratio of pulse on to off	on2off	0.300
duration of smoothing	smooth	0.100 ms
frequency of pulse train (Hz)	freq	$20.00\ s^{-1}$

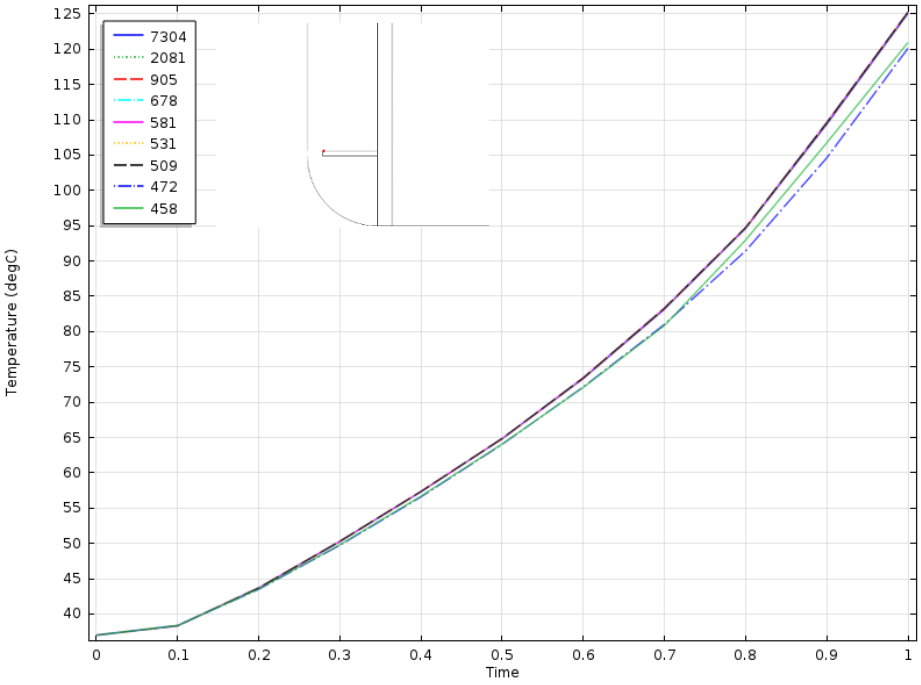

Figure A1. Entire temperature vs. time plot for the depicted point (inside the targeted tissue area near the heat flux surface) used for mesh convergence. This plot converged at a “coarser” mesh with a total of 509 mesh elements.

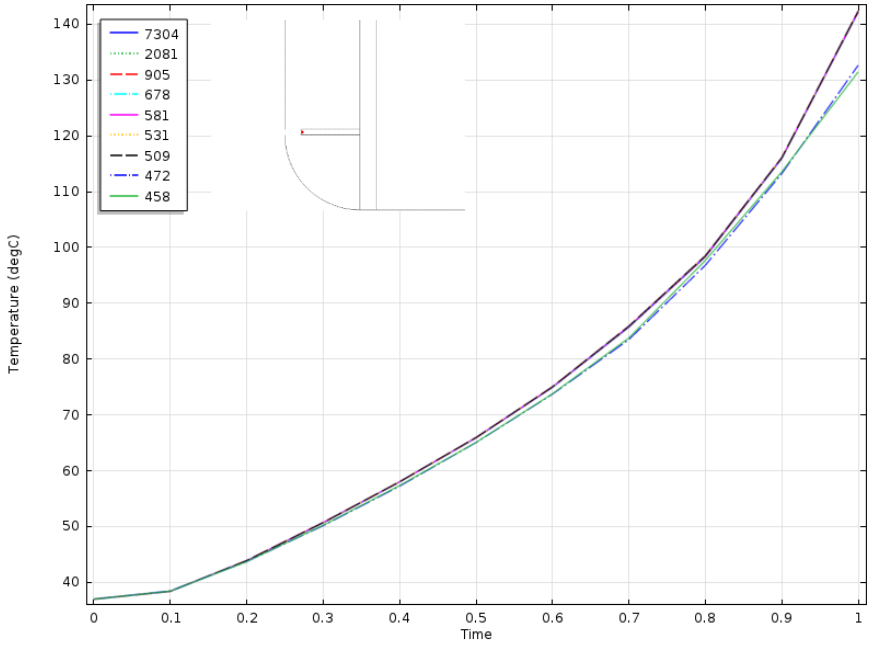

Figure A2. Entire temperature vs. time plot for the depicted point (inside the targeted tissue area near the heat flux surface) used for mesh convergence. This plot converged at a “coarser” mesh with a total of 509 mesh elements.

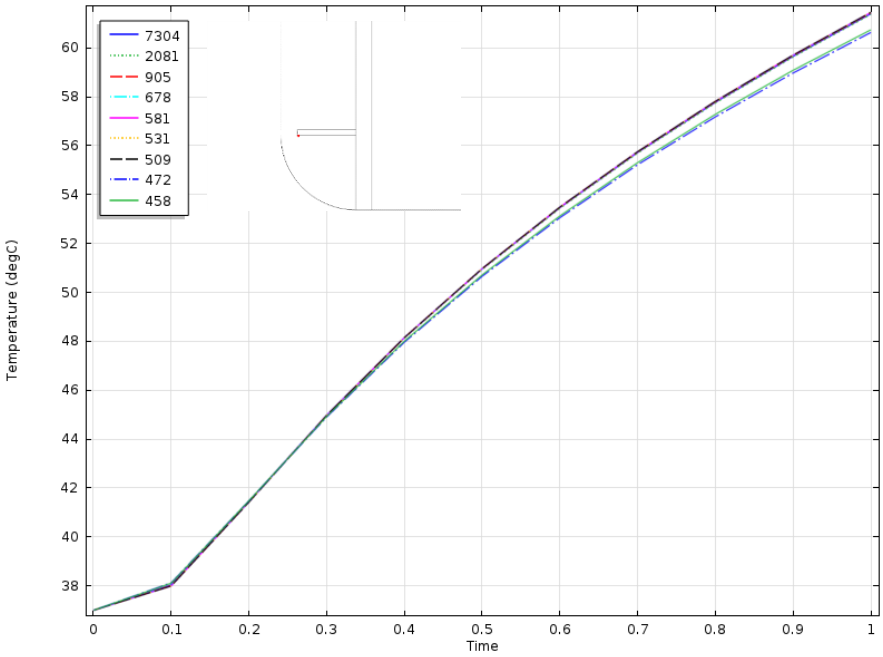

Figure A3. Entire temperature vs. time plot for the depicted point (outside the targeted tissue area, below the incision line and near the heat flux surface) used for mesh convergence. This plot converged at a “coarser” mesh with a total of 509 mesh elements.

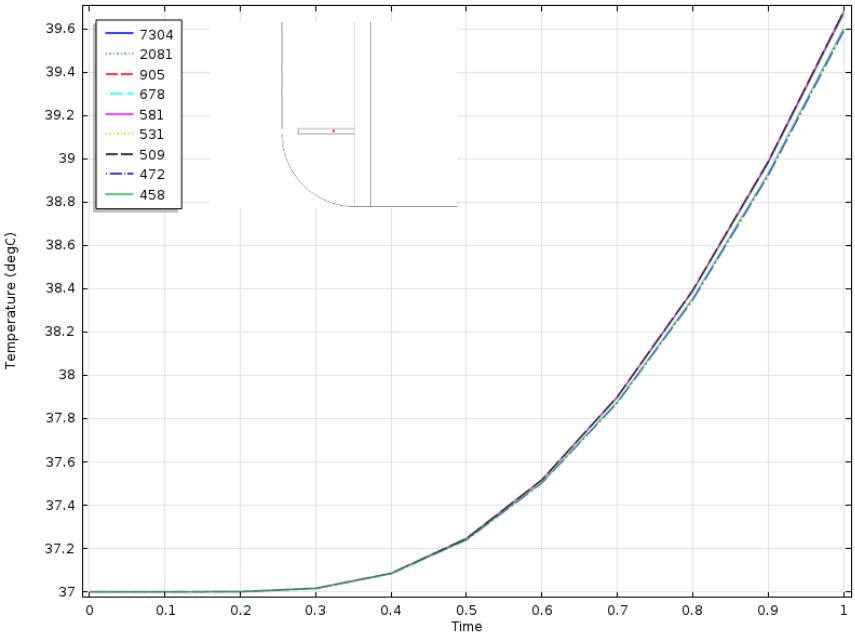

Figure A4. Entire temperature vs. time plot for the depicted point (inside the targeted tissue area) used for mesh convergence. This plot converged at a “coarser” mesh with a total of 509 mesh elements.

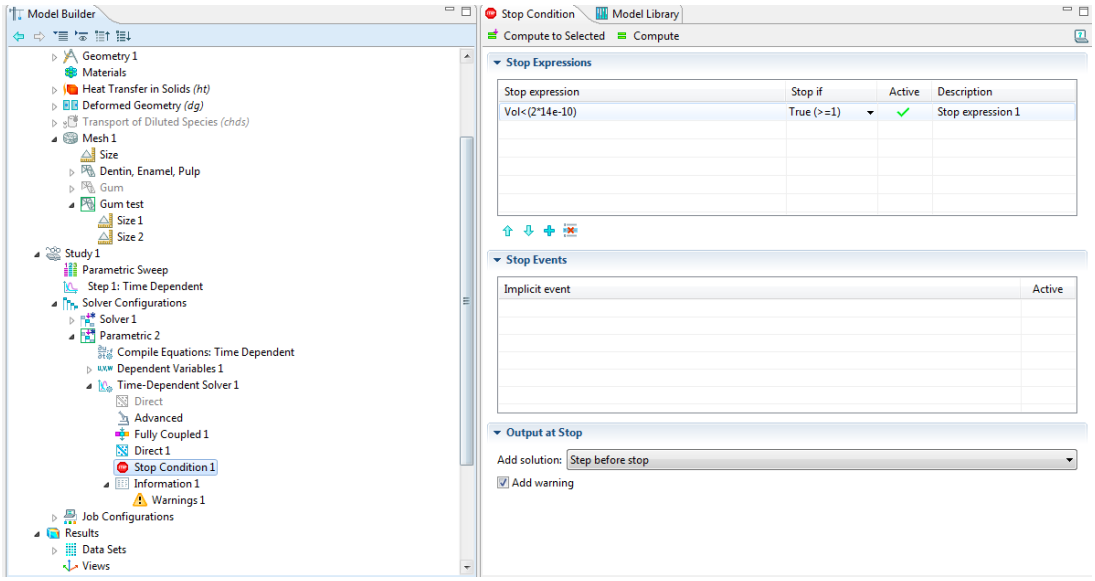

Figure A5. Example of the Stop Condition implemented in the Time Dependent Solver node of the Parametric Solver. Vol integrates the area of the ablated region through another function.

Appendix B:

Ellexion page numbers, drawn from [5]:
Laser temporal pulse generation – 14
Denaturation and Vaporization temperatures – 17
Gingivectomy settings Claros C9, I2 – 79, 81
Gingivectomy settings Duros/Delos C9, I2, P2, P3 – 85, 87

References:

[1] D.M. Sarvar, "Use of the 810 nm diode laser: soft tissue management and orthodontic applications of innovative technology," Pract. Proced. Aesthet. Dent., vol. 19, no. 9, pp. 7-13, 2006. Retrieved from: http://sarvercourses.com/Portals/0/pdfs/diodelaser.pdf

[2] D.F. Salisbury, "Visible and ultraviolet lasers cut flesh by creating a series of overlapping micro-explosions," 2007. Retrieved from: http://www.vanderbilt.edu/exploration/text/index.php?action=view_section&id=1345&story_id=324&images=

[3] B. Cox, "MPHY3886, MPHYM886, MPHYG886 Optics in Medicine. Introduction to Laser-Tissue Interactions," 2013. Retrieved from: http://www.ucl.ac.uk/medphys/staff/people/bcox/BenCox_LaserTissueInteractions.pdf

[4] P. Viraparia et al., " CO2 Laser: Evidence Based Applications in Dentistry," CO2 Laser: Optimisation and Application, 1 ed., Ed. Dr. Dan C. Dumitras, Online.: InTech, 2012, pp. 379-386. Retrieved from: http://cdn.intechopen.com/pdfs-wm/32645.pdf

[5] elexxion, *The Use of Lasers in Dentistry A Clinical Reference Guide for the Diode 810 nm & Er:Yag*. elexxion, 2009.

[6] fmolhs.org "Oral cancer Symptoms & Treatment in - Baton Rouge, LA - Franciscan Missionaries of Our Lady Health System" [Online.] Available: https://ssl.adam.com/graphics/images/en/8880.jpg [Accessed: May 3, 2014.]

[7] puresmile.com. [Online.] Available: http://puresmile.com/wp-content/uploads/2012/03/probclass2.jpg [Accessed: May 5, 2014.]

[8] G.D. Goaslind et al., "Thickness of facial gingiva," J Periodontol., vol. 48, pp. 768-771, 1977.

[9] J.H. de Vree et al., "A simulation model for transient thermal analysis of restored teeth," J Dent Res, vol. 62, pp. 756-759, 1983.

[10] W.S. Brown, "Thermal Properties of Teeth," J Dent Res, vol. 49, pp. 752-755, 1970.

[11] R.G. Craig and F.A. Peyton, "Thermal conductivity of tooth structure, dental cements and amalgam," J Dent Res, vol. 40, pp. 411-417, 1961.

[12] M.C. Haytac et al., " Combined treatment approach of gingivectomy and CO2 laser for cyclosporine-induced gingival overgrowth," Quintessence Int, vol. 38, no. 11, pp. 54-59, 2007.

[13] "DENTA 2 Intraoral Soft Tissue Dental Laser from GPT, Inc. | Dentalcompare: Top Products. Best Practices." Dentalcompare.com. [Online]. Available: http://www.dentalcompare.com/5000-Soft-Tissue-Laser-Dental-CO2-Laser/33259-Lutronic-Spectra-DENTA-CO2/?ncatid=5000&ppim=33259_3_0 [Accessed: May 3, 2014].

[14] "Gingivectomy" YouTube. n.d. [Online] Available:

https://www.youtube.com/watch?v=-z70Xzyi4hc

[15] Chu, J, "Range and mean distribution frequency of individual tooth width of the maxillary anterior dentition," Pract Proced Aesthet Dent vol. 19, no. 4, pp. 209-215, 2007.

[16] greatlaser.com [Online.] Available: http://www.greatlaser.com/CO2-Medical-Laser-System/fractional-co2-laser.htm [Accessed: May 5, 2014.]